Received: 10 July 2017 | Revised: 9 January 2018 | Accepted: 10 January 2018
DOI: 10.1002/ardp.201700223

FULL PAPER

DPhG ARCH PHARM
Archiv der Pharmazie

Synthesis, docking, *in vitro* and *in vivo* antidiabetic activity of pyrazole-based 2,4-thiazolidinedione derivatives as PPAR-γ modulators

Mohd. Javed Naim[1] | **Ozair Alam**[1] | **Md. Jahangir Alam**[1] | **Mohammad Shaquiquzzaman**[1] | **Md. Mumtaz Alam**[1] | **Vegi Ganga Modi Naidu**[2]

[1] Medicinal Chemistry and Molecular Modelling Lab, Department of Pharmaceutical Chemistry, School of Pharmaceutical Education and Research, Jamia Hamdard, New Delhi, India

[2] Department of Pharmacology and Toxicology, National Institute of Pharmaceutical Education and Research, Hyderabad, India

Correspondence
Dr. Ozair Alam, Medicinal Chemistry and Molecular Modelling Lab, Department of Pharmaceutical Chemistry, School of Pharmaceutical Education and Research, Jamia Hamdard, New Delhi-110062, India.
Email: dr.ozairalam@gmail.com

Funding information
DST-SERB, New Delhi, Grant number: SB/FT/LS-203-2012

Abstract

The design, synthesis, structure–activity relationship, and biological activity of 2,4-thiazolidinedione derivatives as peroxisome proliferator-activated receptor-γ (PPAR-γ) modulators for antidiabetic activity are reported. Fifteen 2,4-thiazolidinedione derivatives clubbed with pyrazole moiety were docked into the ligand binding domain of PPAR-γ by the Glide XP module of Schrodinger. Eight derivatives (**5a**, **5b**, **5d**, **5f**, **5i**, **5l**, **5n**, **5o**) having Glide XP scores > −8 as compared to the standard drug, rosiglitazone (Glide XP score = −9.165), showed almost similar interaction with the amino acids such as HIS 449, TYR 473, TYR 327, HIS 323, and SER 289 in the molecular docking studies. These eight derivatives were further screened for PPAR-γ transactivation and *in vivo* blood glucose lowering activity in the streptozotocin-induced diabetic rat model. Compounds **5o**, **5n**, **5a**, **5i**, and **5b** showed 52.06, 51.30, 48.65, 43.13, and 40.36% PPAR-γ transactivation as compared to the reference drugs rosiglitazone and pioglitazone with 85.30 and 65.22% transactivation, respectively. The data analysis showed significant blood glucose lowering effects (hypoglycemia) of compounds **5o**, **5n**, and **5a** (140.1 ± 4.36, 141.4 ± 6.15, and 150.7 ± 4.15, respectively), along with reference drugs pioglitazone (135.2 ± 4.91) and rosiglitazone (141.1 ± 5.88) as compared to the diabetic control. Furthermore, the most potent compound **5o** also elevated the PPAR-γ gene expression by 2.35-fold as compared to rosiglitazone (1.27-fold) and pioglitazone (1.6-fold). It also significantly lowered the AST, ALT, and ALP levels and caused no damage to the liver.

KEYWORDS
diabetes, molecular docking, PPAR-γ, thiazolidinedione

1 | INTRODUCTION

Diabetes has reached an epidemic level by becoming a major health issue round the globe.[1] Peroxisome proliferator-activated receptor-γ (PPAR-γ) agonists have come up with a leading role as an orally effective antidiabetic agent.[2] Diabetes or diabetes mellitus is a multifactorial metabolic disease/polygenic disorder characterized by increased glucose levels/insulin resistance over prolonged periods in

Abbreviations: 15-PGDH, 15-hydroxyprostaglandin dehydrogenase; ALP, alkaline phosphatase; ALT, alanine transaminase; AMPK, 5′-adenosine monophosphate-activated protein kinase; AST, aspartate transaminase; DMEM, Dulbecco's Modified Eagle's Medium; DMF, *N*,*N*-dimethyl formamide; ESI-MS, electrospray ionization mass spectrometry; FBS, fetal bovine serum; FFA, free fatty acid; FT-IR, Fourier transform infrared spectroscopy; HEK, human embryonic kidney; IRAD, insulin resistance associated disorders; LBD, ligand binding domain; mRNA, messenger RNA; NIDDM, non-insulin dependent diabetes mellitus; NMR, nuclear magnetic resonance; PCR, polymerase chain reaction; $POCl_3$, phosphoryl oxychloride; PPAR, peroxisome proliferator-activated receptor; SAR, structure–activity relationship; STZ, streptozotocin; TZD, thiazolidinedione; US FDA, Food and Drug Administration of the United States.

liver and peripheral tissues.[3] It is categorized as Type I, Type II, and gestational diabetes.[4] Type II diabetes (non-insulin-dependent diabetes mellitus) occurs in 80–90% of the patients,[5] often characterized by hyperglycemia and insulin resistance in the initial stages leading finally to serious complications such as stroke, cardiovascular diseases, atherosclerosis, chronic eye damage, kidney failure, obesity, etc.[6–8] collectively known as insulin resistance associated disorders (IRAD).[9]

Glitazones (TZDs or thiazolidinediones), a new class of drug was approved by US FDA in late 1990s for treatment of diabetes which shares common partial structures (rosiglitazone and pioglitazone) and by mid-1990s PPAR-γ was found to be molecular target of these glitazones (Figure 1). Thiazolidinedione (TZD) is an important class of anti-diabetic agent that has attracted attention round the globe for its excellent anti-hyperglycemic profile without causing hypoglycemia. It exhibits a diverse biological profile which includes anti-hyperglycemic,[10] anti-proliferative,[11] antitumor,[12] antioxidant,[13] antimicrobial,[14] anti-inflammatory,[15] antimalarial,[16] cytotoxic,[17] 15-PGDH inhibitors,[18] aldose reductase inhibitor,[19] anti-obesity,[20] histone deacetylase inhibitor,[21] tyrosinase inhibitor,[22] and GPR40 agonist.[23] They have been considered as the high affinity agonist of PPARs (peroxisome proliferator-activated receptors) with maximum selectivity for PPAR-γ instead of PPAR-α and PPAR-β. PPAR-γ also known as glitazone receptor belongs to nuclear receptor family (NR1C3) which regulates the expression of genes involved in glucose metabolism. PPAR-γ is a significant element in adipogenesis which also plays an important role in insulin sensitivity, cell cycle regulation, and cell differentiation. It is the most widely studied PPAR subtype which is further classified as PPAR-γ agonists, PPAR-γ partial agonists, PPAR-α/γ dual agonists, and PPAR-γ antagonists.[24–27] In recent years, we have seen exhaustive research on TZD moiety as an excellent antidiabetic agent due to its attractive features of improving insulin sensitivity and lack of hypoglycemia. However, despite their excellent therapeutic effect, they possess many deleterious target-related side effects which includes weight gain, risk of congestive heart failure, peripheral edema, and increased chances of bone-related disorders. These safety concerns have not only restricted clinical use of these PPAR-γ agonists but also led to failed development of many agonists. Some of the marketed drugs include ciglitazone, troglitazone, pioglitazone, and rosiglitazone of which troglitazone was removed due to its hepatotoxicity.[28] Now new TZD derivatives are being worked on to overcome this complication[29–31] for which we hunt surrogate lipophilic templates to take over larger lipophilic core of earlier representative agonists. Furthermore the PPAR-γ LBD (ligand-binding domain) is Y-shaped cavity and the docking studies of new lead (compound, **5o**) efficiently fill this cavity.[32] This approach has led to convincing improvement of PPAR-γ activity. Further optimization to balance *in vitro* activity and metabolic stability allowed the discovery of selective, potential, and orally efficacious PPAR-γ agonist. Structure–activity relationship (SAR) study as well as thorough exploration of the binding mode of compounds to the PPAR-γ-LBD revealed the necessary structural features of these lead molecules as mentioned in Figure 1. The central phenyl ring of pioglitazone and rosiglitazone is replaced by pyrazole ring which was then attached with the TZD ring through the linker. Further a lipophilic fragment was directly attached (without having the oxymethyl linker as in the pioglitazone and rosiglitazone) to the central pyrazole, and another phenyl group was attached through N-1 atom of the pyrazole in such a way that the designed molecules can efficiently accommodate in the Y-shaped PPAR-γ-LBD. Here, we report the design and synthesis of newer 2,4-thiazolidinedione derivatives (**5a–o**), which were then evaluated for *in vitro* PPAR-γ transactivation and gene expression studies and *in vivo* blood glucose lowering and hepatotoxicity studies with a hope to overcome the complications/side effects as reported in earlier marketed drugs. The derivatives (**5a–o**) were then characterized by ^{1}H NMR, ^{13}C NMR, IR and mass spectral analysis.

2 | RESULTS AND DISCUSSION

2.1 | Chemistry

The title compounds **5a–o** were synthesized as per the route outlined in Scheme 1. The compounds **3a–o** were synthesized by treating substituted acetophenones/aryl ketones (**1a–o**) with phenyl hydrazine (**2**) which then undergoes Vilsmeier–Haack reaction in the presence of $POCl_3$ and *N*,*N*-dimethyl formamide (DMF) to give pyrazole carbaldehydes **4a–o**. These resulting carbaldehydes were finally treated with 2,4-thiazolidinedione to give the final derivatives **5a–o**. The structures of TZD derivatives (**5a–o**) were characterized by FT-IR, ^{1}H and ^{13}C NMR (Bruker-400 NMR spectrometers) and mass spectrometry (ESI-MS, water). Elemental analysis (C, H, and N) data were within ±0.4% of the theoretical values. The formation of TZD derivatives was confirmed by the appearance of a singlet for —CHC— protons at δ 7.607–8.311 ppm and a broad singlet for NH-TZD protons at δ 12.337–12.564 in ^{1}H NMR spectra followed by the presence of peaks 3347–3379 cm^{-1} (NH_{str}), 1723–1773 ($C{=}O_{str}$), 1649–1681 ($—CH{=}C_{str}$), 1548–1582 ($C{=}N_{str}$), and 642–679 (C—S) in the IR spectrum.

2.2 | Pharmacological activities

2.2.1 | *In vitro* PPAR-γ transactivation assay

The derivatives with good Glide scores (>8) in molecular docking studies were further screened for PPAR-γ transactivation assay so as to determine their mode of action as compared to the reference drug rosiglitazone with a Glide score of −9.165. Compounds **5a**, **5b**, **5i**, **5n**, and **5o** were found to be PPAR-γ active. Compounds **5o**, **5n**, **5a**, **5i**, and **5b** showed 52.06, 51.30, 48.65, 43.13, and 40.36% PPAR-γ transactivation as compared to reference drugs rosiglitazone and pioglitazone with 85.30 and 65.22% transactivation, respectively, while compounds **5d**, **5f**, and **5l** showed moderate results (Figure 2).

2.2.2 | *In vivo* blood glucose lowering effect

Streptozotocin (STZ)-induced diabetic model is the most preferred model because of its lengthier half-life and hyperglycemic interval

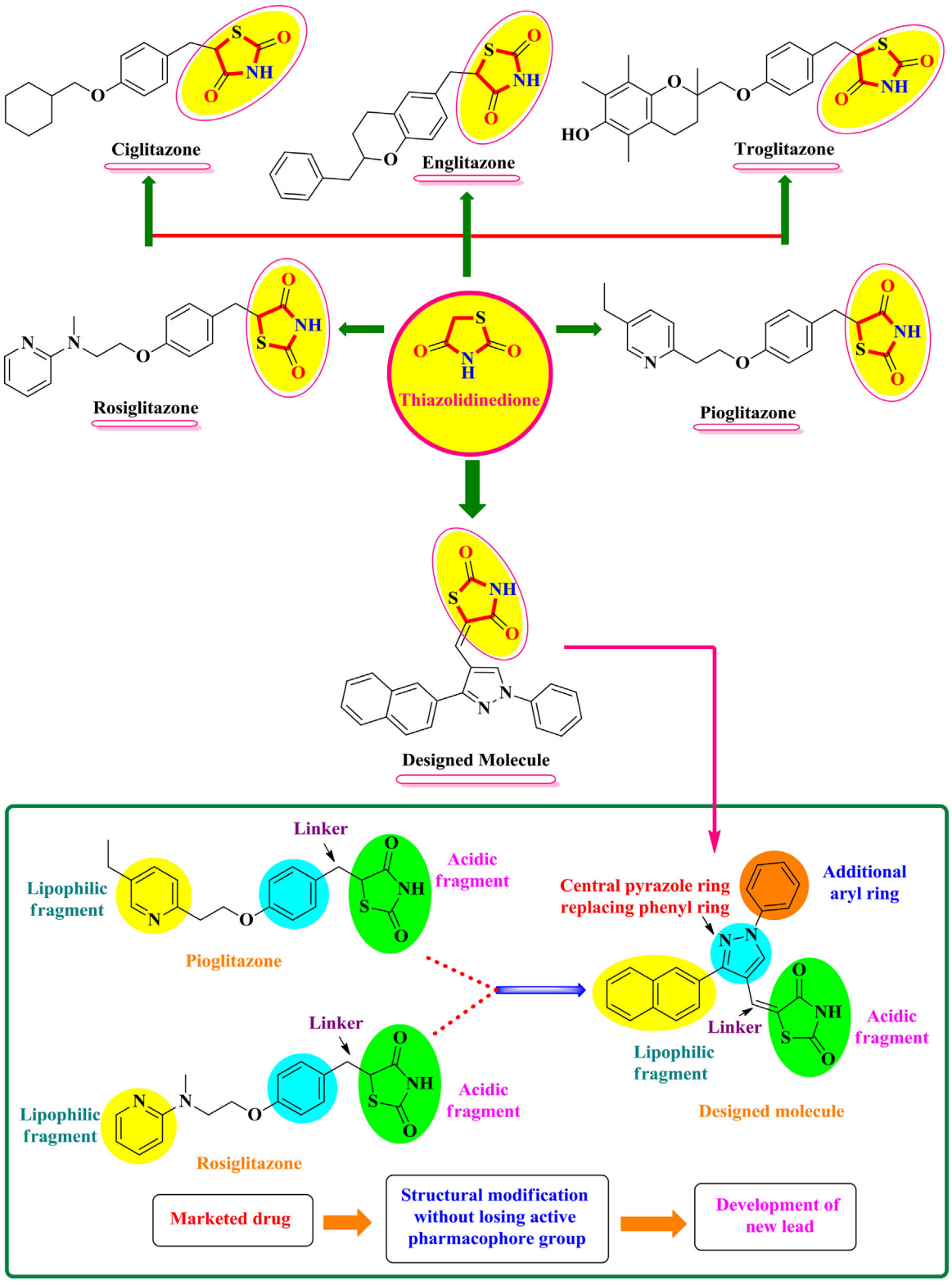

FIGURE 1 Reported thiazolidinedione containing derivatives showing anti-diabetic activity along with designed molecule

followed by reduced risk of ketosis and mortality. The TZD derivatives **5a**, **5b**, **5d**, **5f**, **5i**, **5l**, **5n**, and **5o** were evaluated on STZ-induced diabetic rats for their blood glucose lowering effect. A single dose of these compounds was administered and the blood glucose levels were monitored as per standard protocols on 1st, 7th, and 15th day of the commencement of experiment. The data analysis showed significant blood glucose lowering effect (hypoglycemia) with compounds **5o**, **5n**, and **5a** showing 140.1 ± 4.36, 141.4 ± 6.15, and 150.7 ± 4.15, respectively, along with reference drugs pioglitazone (135.2 ± 4.91) and rosiglitazone (141.1 ± 5.88) as compared to diabetic control. Therefore

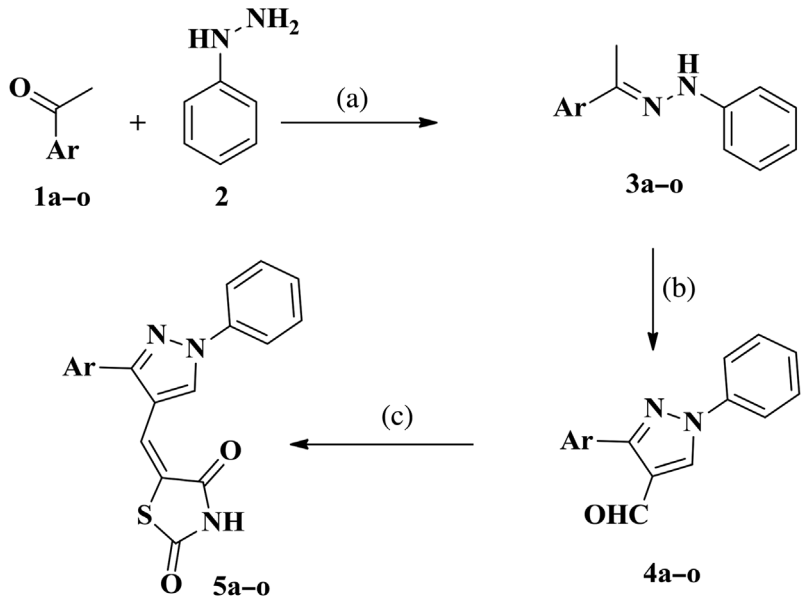

Comp.	Ar	Comp.	Ar	Comp.	Ar
5a	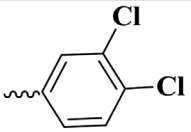	5f	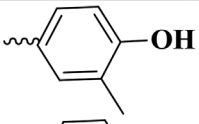	5k	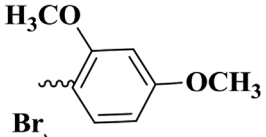
5b	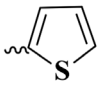	5g	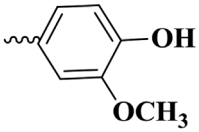	5l	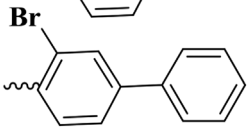
5c	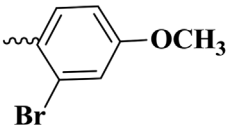	5h	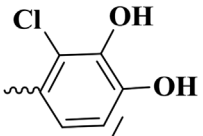	5m	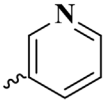
5d	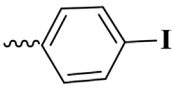	5i	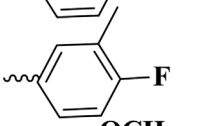	5n	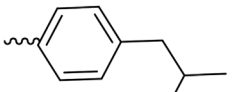
5e	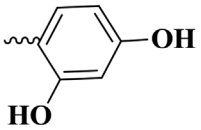	5j	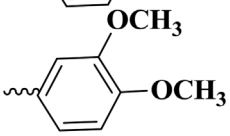	5o	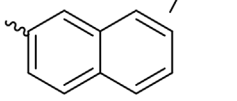

SCHEME 1 Reagents and conditions: (a) Abs. ethanol, conc. HCl, reflux for 6–8 h; (b) DMF, $POCl_3$, reflux for 6–8 h; (c) TZD, abs. ethanol, piperidine, reflux for 3–5 h

these synthesized compounds showed almost identical blood glucose lowering effect as reference drugs. Compounds **5i** and **5b** showed moderate results whereas compounds **5d**, **5f**, and **5l** were found to be least active as compared to reference drugs (Figure 3).

2.2.3 | Body weight gain study

Compound **5o** was further analyzed for body weight gain study for 15 days. No significant body weight change was observed in **5o**-treated normal rats and normal control rats. However, diabetic rats showed significant improvement in weight gain which is shown in Figure 4.[2]

2.2.4 | Hepatotoxicity studies

The derivatives **5a–o** were synthesized with a view to overcome the reported hepatotoxic effects of TZDs. The compounds with good *in vivo* results **5a**, **5b**, **5i**, **5n**, and **5o** were further analyzed for increase or decrease in the levels of aspartate transaminase (AST), alanine transaminase (ALT), and alkaline phosphatase (ALP) followed by histopathological study of liver. Due to toxic effects of the STZ on rats liver, the level of these enzymes were significantly increased but decreased to almost normal after administration of the respective compounds. The compound **5o** was found to be the most potent in lowering down the levels of AST, ALT, and ALP as compared to

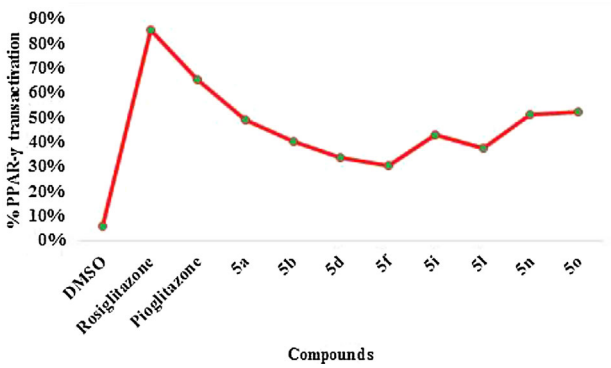

FIGURE 2 *In vitro* PPAR-γ transactivation assay of the compounds. Values are expressed as mean ± SE from three experiments conducted in triplicate at 10 mM

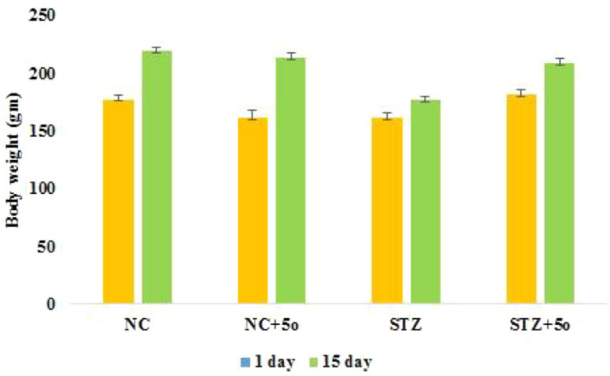

FIGURE 4 Effect of compound **5o** on body weight in albino Wistar rats. Data are analyzed by one-way ANOVA followed by Dunnett's *t*-test and expressed as mean ± SEM from five observations; $^{*}p < 0.01$ versus diabetic control. NC, normal control; NC + **5o**, normal control + **5o**; STZ, diabetic control; STZ ± **5o**, **5o**-treated diabetic rats

pioglitazone. Compounds **5i** and **5b** were found to be equally potent as the reference drug in reducing the level of these enzymes to normal (Figure 5). Histopathological studies also confirmed that **5b**, **5i**, **5n**, and **5o** caused no damage to liver. Compound **5a** was found to decrease the levels of AST and ALT and found to be hepato-protective but in contrast it showed slight dilation of sinusoidal space in microscopical image of the liver (exact mechanism unknown) along with pioglitazone (Figure 6).

2.2.5 | PPAR-γ gene expression study

PPAR-γ gene expression study was carried out to determine the effect of the most potent derivative (**5o**) on PPAR-γ gene. The gene analysis includes compound **5o** and reference drugs rosiglitazone and pioglitazone in 10 μM concentrations and it was observed that the expression of the PPAR-γ gene was significantly increased by 2.35-fold for compound **5o** as compared to the standard drugs rosiglitazone and pioglitazone where expression was increased by 1.27- and 1.6-fold

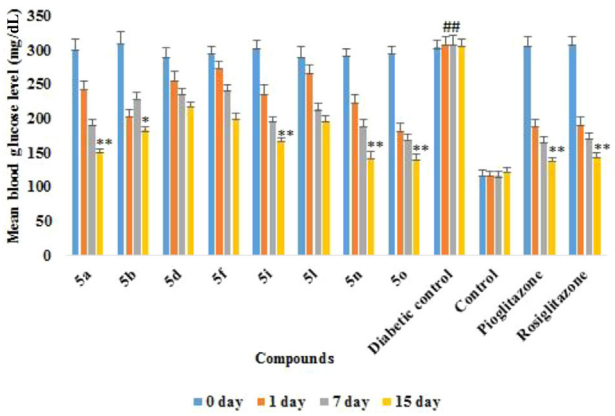

FIGURE 3 Antidiabetic activity of compounds in STZ-induced diabetic rats. Data are analyzed by one-way ANOVA followed by Dunnett's *t*-test and expressed as mean ± SEM from five observations; $^{\#\#}p < 0.01$ versus control; $^{**}p < 0.01$ and $^{*}p < 0.05$ versus diabetic control

(Figure 7). Thus, the increase in gene expression due to compound **5o** supports and is responsible for blood glucose lowering effect and PPAR-γ transactivation. This increase in expression of PPAR-γ genes might be due to AMPK activation. TZDs have been reported to improve action of insulin by effecting gene transcription in fat cells leading to decreased free fatty acids (FFAs) level in plasma followed by increase in adiponectin level. The overexpression of PPAR-γ in 3T3-L1 adipocytes increases mRNA content for ubiquitous GLUT1 which is down regulated during differentiation of adipocytes. The insulin-stimulated glucose transport in 3T3-L1 was found to be reduced due to diminished expression of IR, IRS1, IRS2, and GLUT4. As a result, compound **5o** increases gene expression and levels of GLUT1 and GLUT4 while maintaining insulin sensitivity in mature 3T3-L1 adipocytes.[33,34]

2.3 | Molecular docking

The molecular docking study of the designed and synthesized compounds into the LBD (ligand binding domain) of PPAR-γ was carried out to explore the possible binding interactions as well as to compare the binding pattern of these synthesized compounds to the well-known PPAR-γ modulator, rosiglitazone. The compounds **5a**, **5b**, **5i**, **5n**, and **5o** showing good overall results were then selected for interaction with LBD of PPAR-γ which has a Y-shaped cavity composed of a hydrophobic gate (ARM 3) which is divided into two sub-arms, ARM 1 (essentially polar), which is lengthened toward helix 12 (H 12), and ARM 2 (predominantly hydrophobic), which is placed between helix 3 (H 3) and a β-sheet, as shown in Figure 8.

The molecular docking studies showed that compounds **5a**, **5b**, **5i**, **5n**, and **5o** were well accommodated in the PPAR-γ active site. The compound **5o** interacted well with PPAR-γ-LBD in a manner similar to known PPAR-γ modulator, rosiglitazone. The 3D binding mode of docked compound **5o** showed six hydrogen bond interactions with the

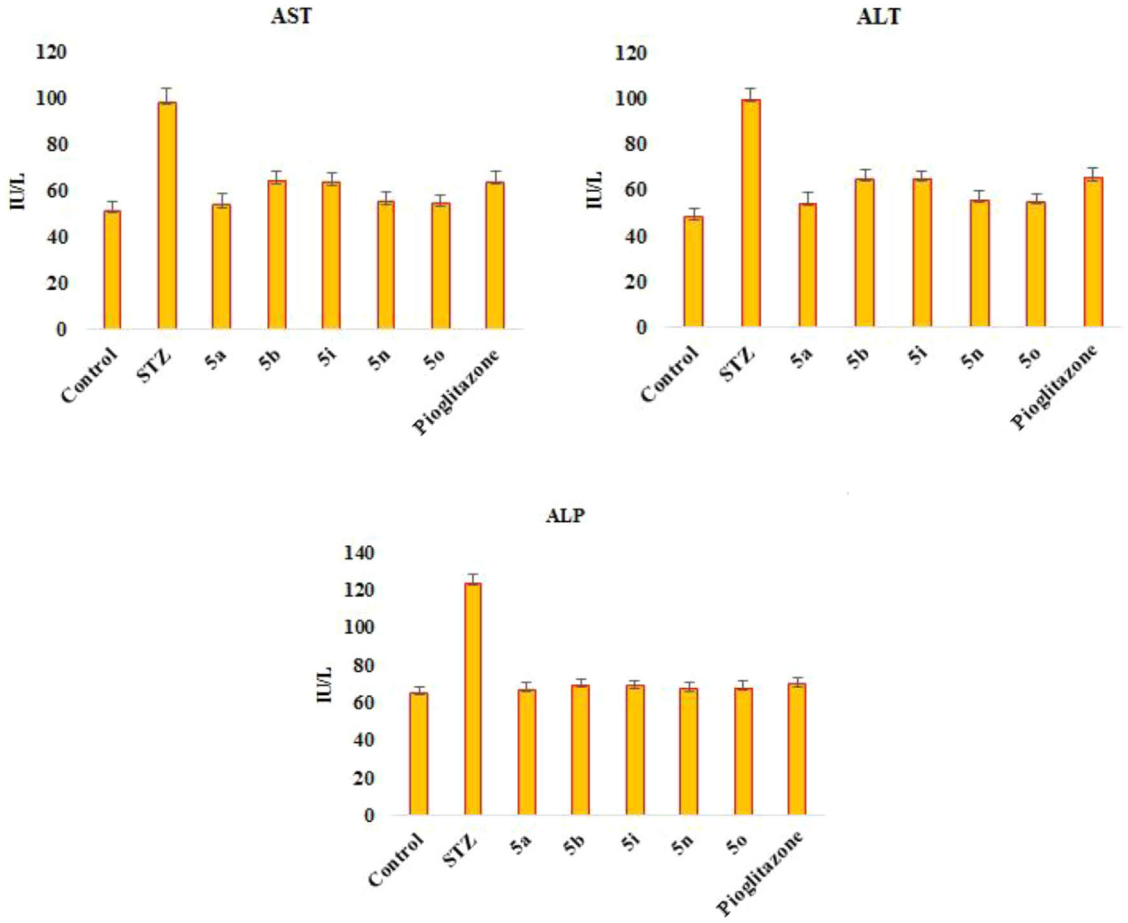

FIGURE 5 Effect of compounds on serum AST, ALT, and ALP activities. Values are given as mean ± SD

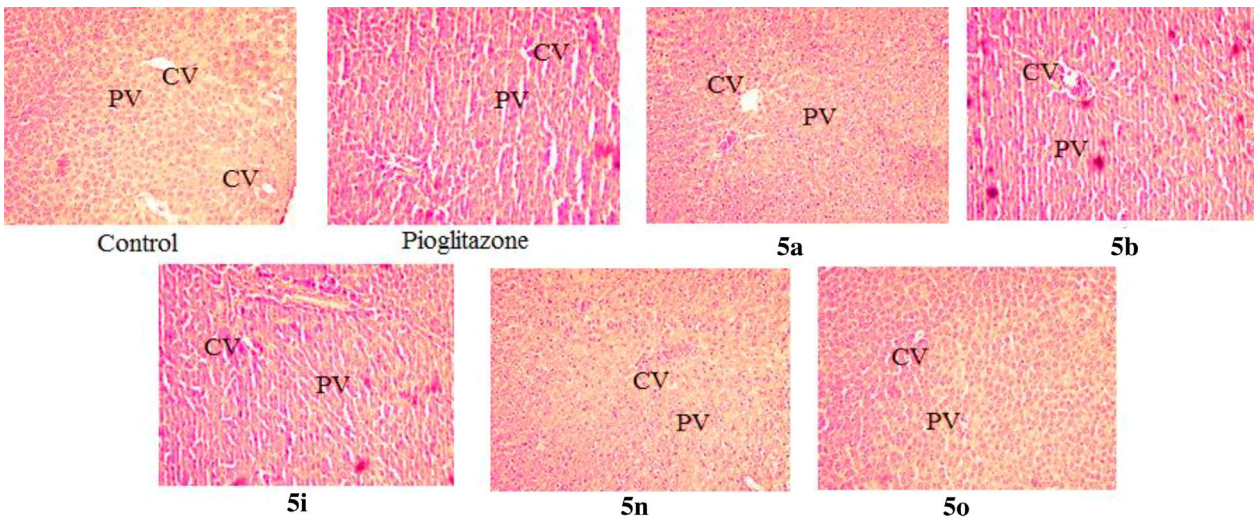

FIGURE 6 Photomicrograph of rat liver stained with hematoxylin and eosin (H & E) is shown in the above figure. Histopathology study of rat liver was illustrated in animal-treated groups **5a**, **5b**, **5i**, **5n**, and **5o**, normal control and standard. Photomicrographs of liver of control group are showing normal arrangement of innumerable lobe and consisting of central vein and portal vein. There were no pathological changes of lobe in group treated with our synthesized drug (**5b**, **5i**, **5n**, and **5o**), when treated groups were compared with the control group. **5a** and pioglitazone-treated groups showed mild dilatation of sinusoidal spaces around the central vein and mild inflammation in portal vein

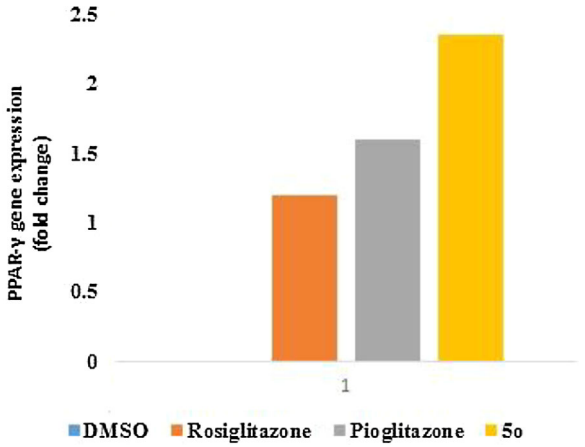

FIGURE 7 Effect of compound **5o** on PPAR-γ gene expression. The experiments were conducted at 10 μM. PCR was performed in triplicate and was repeated two times for each gene and sample. Relative transcript quantities were calculated using the Ct method with β-actin as the endogenous reference gene

side chain residues SER 289 (C═O...HO, 3.03 Å), TYR 327 (C═O...HO, 2.91 Å), HIP 323 (C═O...HN, 3.26 Å), TYR 473 (NH...OH, 3.97 Å), and HIP 449 (CO...HN, 3.86 Å) as displayed in Figure 10a and an additional hydrogen bonding and π-cation interaction with ARG 288 (pyrazole-N...HN, 3.92 Å and phenyl...CN, 4.17 Å, respectively). The hydrophilic acidic head group 2,4-thiazolidinedione ring of compound **5o** binds to AF-2 (activation factor 2) helix to form a network of hydrogen bonds with HIP 449 (Helix 11), TYR 473 (Helix 12), SER 289 (Helix 3), TYR 327 (Helix 4), and HIP 323 (Helix 4), shown in Figure 9 and occupy the right arm of Y-shaped cavity, as shown in Figure 8. These interactions of 2,4-thiazolidinedione ring

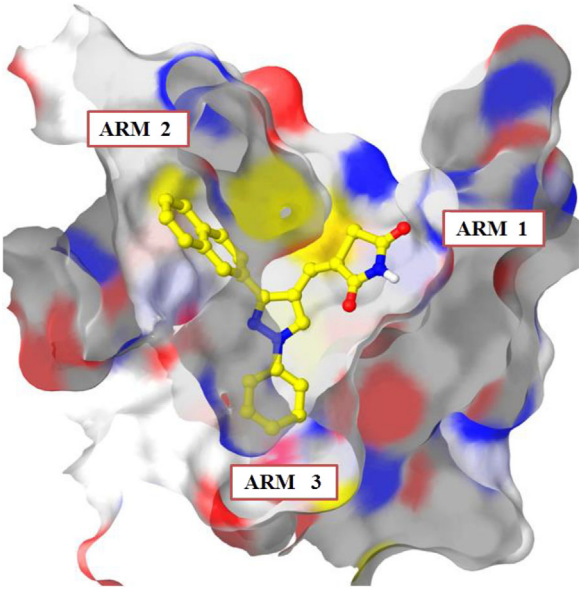

FIGURE 8 Structure of the Y-shaped LBD of PPAR-γ forming a complex with compounds **5o** (yellow color)

FIGURE 9 Insight of the PPAR-γ protein complexes with compounds **5o** (turquoise color) showing interaction with different helixes. The protein is represented as cartoon model

stabilize helix 12 (H12) and are crucial for the transactivation activity as well as agonistic activity of PPAR-γ. Compound **5n** binds with the acidic TZD moiety in a fashion similar to that observed in compound **5o** and showed hydrogen bonding with SER 289 (C═O...HO, 2.99 Å), TYR 327 (NH...OH, 3.05 Å), HIP 323 (C═O...HN, 3.00 Å), TYR 473 (NH...OH, 3.56 Å), and HIP 449 (C═O...HN, 3.74 Å), as shown in Figure 8b. Moreover, **5n** also forms additional hydrogen bonding with ARG 288 (pyrazole-N...HN, 3.98 Å). However, the TZD moiety of compounds **5a** and **5i** as shown in Figure 10c and d interacted with the PPAR-γ in a similar fashion as **5o**. Compound **5a** binds to the LBD of PPAR-γ through hydrogen bonding with SER 289 (C═O...HO, 3.00 Å), TYR 327 (NH...OH, 2.89 Å), HIP 323 (C═O...HN, 3.17 Å), TYR 473 (NH...OH, 3.76 Å), and HIP 449 (C═O...HN, 3.95 Å), as shown in Figure 10c. In addition, **5a** also forms hydrogen bonding with ARG 288 (pyrazole-N...HN, 3.88 Å). Compound **5i** (containing the *meta* methyl and *para* fluoro group) forms a network of hydrogen bonds with SER 289 (C═O...HO, 3.03 Å), TYR 327 (NH...OH, 2.86 Å), HIP 323 (C═O...HN, 3.19 Å), TYR 473 (NH...OH, 3.79 Å), and HIP 449 (C═O...HN, 3.96 Å), as shown in Figure 10d whereas the pyrazole ring in **5i** formed a hydrogen bond with ARG 288 (pyrazole-N...HN, 3.92 Å).

It was clearly observed that compounds containing small heterocyclic ring such as thiophene (**5b**) attached to the pyrazole scaffold enhances the interaction of TZD moiety to TYR 473, on the other hand **5b** also formed a π–π interaction with TYR 327 (thiophene...phenyl, 4.86 Å). The acidic TZD moiety of compound **5b** fitted nicely into the LBD site of the PPAR-γ making five hydrogen bond interactions with HIP 449 (C═O...HN, 2.81 Å), GLN 286

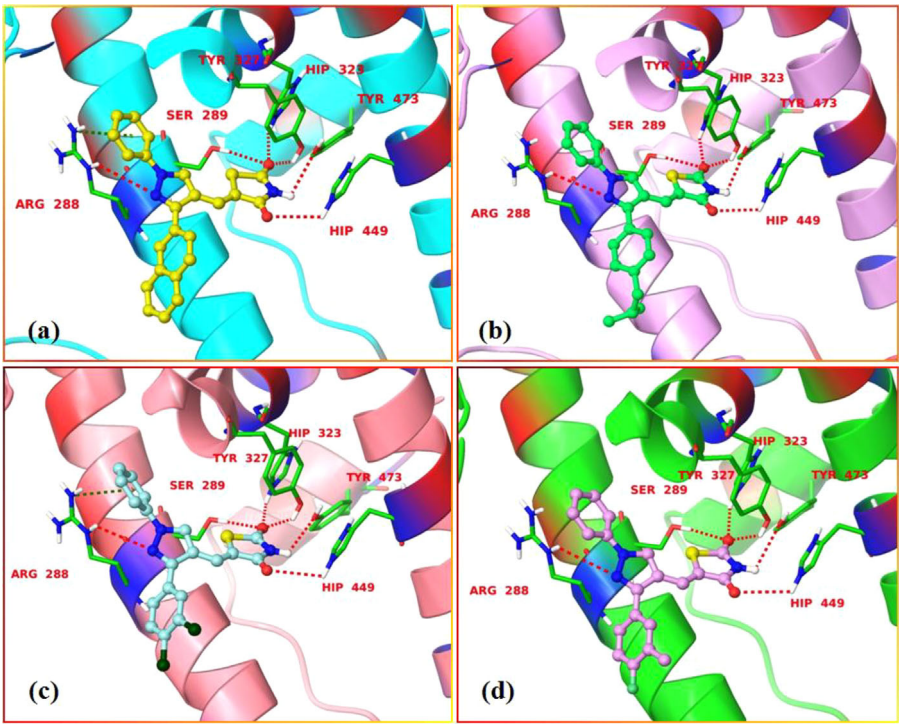

FIGURE 10 Docked pose of compounds (a) **5o** (yellow color), (b) **5n** (green color), (c) **5a** (turquoise color), and (d) **5i** (plum color) showing hydrogen bond interaction (red-dashed lines) with amino acids in the binding site of PPAR-γ. The ligand and amino acids are represented as ball and stick and tube model, respectively

(C═O...H_2N, 2.33 Å), TYR 473 (NH...OH, 3.52 Å), HIP 323 (CO...HN, 1.67 Å), and SER 289 (C═O...HO, 1.77 Å) as shown in Figure 11a. The receptor surface model of compound **5o** in the binding site of PPAR-γ is also depicted in Figure 11b. It was established that the compounds having bulkier hydrophobic moiety/group such as naphthalene and isobutyl phenyl were the most active in the series. The co-crystal ligand, rosiglitazone assumed to occupy the LBD of PPAR-γ and established hydrogen bonding interactions with HIP 323, SER 289, TYR 327, TYR47, HIP 449, and GLN 286, as depicted in Figure 12a. The docked compound **5o** superimposed well with the co-crystal ligand rosiglitazone and all common interactions (HIP 449, TYR 473, HIP 323, TYR 327, and SER 289) were consistent with the ones in the crystal complexes of ligand binding domain (LBD) of PPAR-γ, as shown in Figure 12b. The **5o** derivative is enclosed by hydrophobic amino acids such as ILE 326, TYR 327, LEU 330, VAL 339, ILE 341, LEU 353, ILE 281, and PHE 363 shown in Figure 13a, while co-crystal ligand rosiglitazone is surrounded by hydrophobic amino acids such as ILE 281, LEU 353, VAL 339, and ILE 341, represented in Figure 13b.

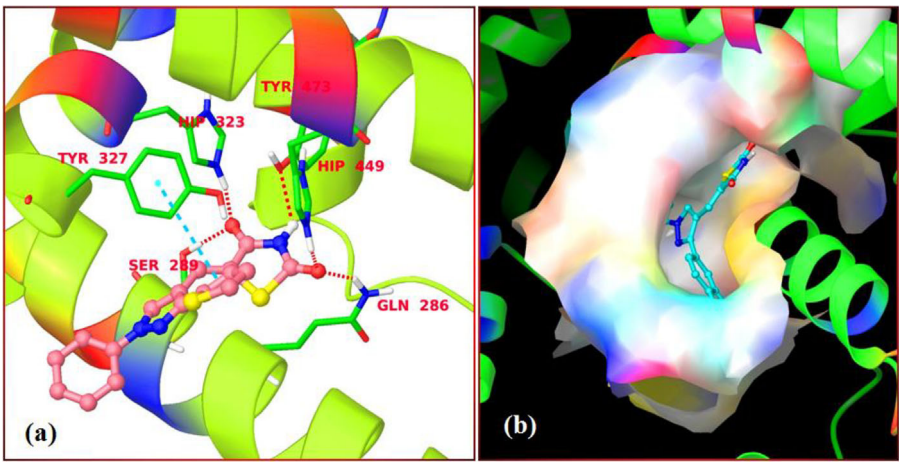

FIGURE 11 (a) Docked pose of **5b** (plum color) showing hydrogen bond interaction (red-dashed lines) with amino acids in the binding site of PPAR-γ. (b) Receptor surface model of **5o** (turquoise color) in the binding site of PPAR-γ

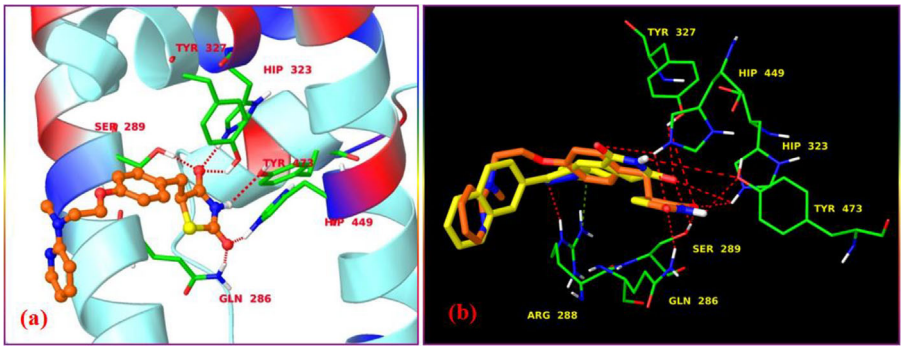

FIGURE 12 (a) Docked pose of rosiglitazone showing hydrogen bond interaction (red-dashed lines) with amino acids in the binding site of PPAR-γ. (b) Superimposed structure of compound **5o** (turquoise color) with rosiglitazone (yellow color) at the binding site of PPAR-γ

The molecular docking protocol was validated by re-docking of the co-crystallized ligand rosiglitazone back into the same active site of PPAR-γ and found to follow the same interaction pattern and results with RMSD value of 1.9 and, therefore, docking protocol was validated by the generated grid. The information achieved from this work must be useful to compare the binding modes of designed compound **5o** to the known PPAR-γ modulator, i.e., rosiglitazone and pioglitazone, and expedient for further designing and development of newer PPAR-γ modulators with advantages over current marketed TZD derivatives.

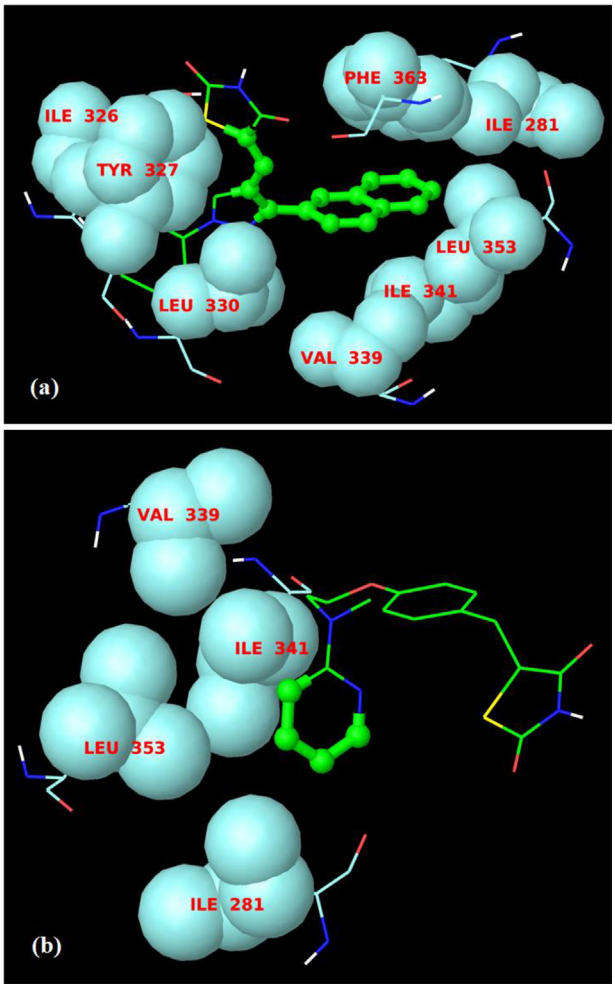

FIGURE 13 XP visualization pose of (a) compound **5o** and (b) rosiglitazone, showing major hydrophobic interactions with the PPAR-γ LBD

2.4 | SAR

The SAR of the derivatives in relation to PPAR-γ transactivation revealed that compounds containing bulkier aryl groups at N-position of the pyrazole core as in **5n** (51.30%) and **5o** (52.06%) showed good *in vitro* results. Introduction of a halo atom at the phenyl ring resulted in enhanced antidiabetic activity. Among the halo derivatives, di-substitutions at the *meta* and *para* positions in **5a** (48.65%) showed significant lowering in blood glucose level than halogen at other positions. Compounds **5i** (43.13%) with smaller halogen atom F at *para* position and an electron releasing group (methyl group) at *meta* position was found more potent than the larger bromo derivatives. The replacement of aromatic ring with thiophene in **5b** (40.36%) resulted in moderate activity, despite having marginally poor aromatic character and very good interaction of thiophene ring with the PPAR-γ receptor. However, compound **5l** showed moderate activity due to steric hindrance caused by the larger size of the 2-bromo biphenyl group. Compound **5f** containing electron releasing group at *meta* and *para* positions on the aryl ring observed less lowering in blood glucose level. Interestingly, incorporation of an additional methyl group at the *meta* position along with *para* fluoro in compound **5i** was also able to produce significant lowering in blood glucose with respect to compound **5f** having methyl group at *meta* position and hydroxyl at *para* position on aryl ring. Compound **5d**, with the larger iodo group in the *para* position of phenyl ring demonstrated low activity.

3 | CONCLUSION

A series of 15 TZD derivatives have been synthesized among which compounds **5a**, **5b**, **5i**, **5n**, and **5o** exhibited significant *in vitro* PPAR-γ transactivation and *in vivo* antidiabetic potency. Among these derivatives, compound **5o** (equipped with naphthalene moiety)

appeared as the most potential antidiabetic agent with no noteworthy weight gain and showed no signs of hepatotoxicity. Compound **5o** exhibited 2.35-fold increase in PPAR-γ gene expression against pioglitazone (1.6-fold) and rosiglitazone (1.27-fold) as standard drugs. Compound **5o** may be considered as a potential and safe candidate which may undergo modifications for the design and development of newer antidiabetic agents/PPAR-γ modulator.

4 | EXPERIMENTAL

4.1 | Chemistry

4.1.1 | General

All required chemicals, solvents, and reagents were purchased from Sigma–Aldrich and Merck India. Progress of the reaction was monitored on pre-coated thin layer chromatographic aluminum sheets Silica Gel Merck 60 F254 (Merck) using toluene/ethyl acetate/formic acid (5:4:1), benzene/acetone (8:2) and TLC spot visualization was done by using UV lamp and iodine chamber. Melting points of the synthesized compounds were determined by open glass capillary tubes and are uncorrected. Fourier transform infrared spectra were recorded on (IR Affinity SHIMADZU) FTIR-spectrophotometer using KBr pellets and λ_{max} values were given in cm^{-1}. The ^1H NMR and ^{13}C NMR spectra were recorded on Bruker model DRX-400 and 100 MHz, respectively, in $CDCl_3$ and DMSO-d_6 solvents using tetramethylsilane (TMS) as the internal standard. Chemical shift values are given in δ (ppm) scale and the signals are described as s (singlet), d (doublet), t (triplet), q (quartet), and m (multiplet) whereas coupling constants (*J*) are expressed in Hz. Mass spectra (ESI-MS) were recorded on a Waters mass spectrometer UPLC-MS/MS and elemental analysis was undertaken with Perkin-Elmer model 240C analyzer. Elemental analysis was ±0.4%, i.e. within the theoretical values.

The InChI codes of the investigated compounds are provided as Supporting Information.

4.1.2 | General procedures for the synthesis of TZD derivatives (5a–o)

Synthesis of substituted hydrazones 3a–o

To a solution of (**1a–o**) substituted acetophenones/aryl ketones (0.01 moles) and (**2**) phenyl hydrazine (0.02 moles) in absolute ethanol (25–30 mL) were added few drops of concentrated HCl in a 100 mL round bottom flask and refluxed for 6–7 h. The solvent (abs. ethanol) was evaporated under reduced pressure; the residue left was poured into crushed ice with continuous stirring, filtered, washed with ice cold water, dried, and recrystallized from ethanol.

Synthesis of substituted pyrazole carbaldehydes 4a–o

To a solution of DMF (0.188 mol; ~14.5 mL) at 0–5°C under continuous stirring was added $POCl_3$ (0.0385 mol; ~3.6 mL) slowly drop-wise for 15–20 min (Vilsmeier–Haack reaction). Substituted hydrazone (**3a–o**, 0.00925 mol) was then added and stirred for few minutes and then heated at 70–80°C for 6–8 h. Cool it, pour in minimum amount of crushed ice and basify it with saturated solution of $NaHCO_3$, filtered, dried, and recrystallized from ethanol.[35]

Synthesis of TZD derivatives 5a–o

Equimolar quantities of substituted pyrazole carbaldehydes (**4a–o**) and TZD (earlier prepared from thiourea and chloroacetic acid) in absolute ethanol with few drops of glacial acetic acid and piperidine was refluxed for 2–3 h. The solvent was removed under reduced pressure; residue left behind was poured in crushed ice, filtered, washed with ice cold water, dried, and recrystallized from ethanol to yield the final derivatives[36,37] (Scheme 1).

4.1.3 | Characterization of synthesized compounds

5-((3-(3,4-Dichlorophenyl)-1-phenyl-1*H*-pyrazol-4-yl)-methylene)thiazolidine-2,4-dione (5a)

Yield = 59%, m.p. 256–258°C, R_f = 0.63. FT-IR (KBr, ν_{max} cm^{-1}): 3349 (NH), 3067, 3044 (C—H, Ar), 1751, 1739 (C═O), 1655 (—CH═C—), 1568 (C═N), 1386 (C—N), 775 (C—Cl), 650 (C—S). ^1H NMR ($CDCl_3$, 400 MHz), δ ppm: 7.424–7.443 (t, 1H, Ar—H, *J* = 7.6 Hz), 7.517–7.580 (m, 4H, Ar—H), 7.788–7.797 (m, 3H, Ar—H), 8.073 (s, 1H, —CHC), 8.536 (s, 1H, CH, pyrazole-H), 12.536 (bs, 1H, NH-TZD). ^{13}C NMR ($CDCl_3$, 75 MHz): 114.8, 119.5, 121.1, 123.7, 126.3, 128.1, 128.5, 129.2, 129.7, 130.2, 131.3, 132.9, 139.0, 142.3, 152.3, 167.0, 167.6. ESI-*m/z*: 417.73 $[M+H]^+$. Anal. calcd. for $C_{19}H_{11}Cl_2N_3O_2S$: C, 54.82; H, 2.66; N, 10.09. Found: C, 54.85; H, 2.62; N, 10.13%.

5-((1-Phenyl-3-(thiophen-2-yl)-1*H*-pyrazol-4-yl)methylene)-thiazolidine-2,4-dione (5b)

Yield = 73%, m.p. 230–232°C, R_f = 0.79. FT-IR (KBr, ν_{max} cm^{-1}): 3367 (NH), 3085, 3044 (C—H, Ar), 1767, 1752 (C═O), 1661 (—CHC—), 1579 (CN), 1376 (C—N), 651 (C—S). ^1H NMR (DMSO-d_6, 400 MHz), δ ppm: 7.258–7.269 (t, 1H, *J* = 4.4 Hz, —CH-thiophene), 7.409–7.428 (t, 2H, *J* = 7.6 Hz, —CH-thiophene), 7.555–7.574 (t, 2H, Ar—H, *J* = 7.6 Hz), 7.740–7.750 (d, 2H, Ar—H, *J* = 4 Hz), 7.964–7.984 (m, 2H, Ar—H, —CH═C), 8.681 (s, 1H, CH, pyrazole-H), 12.560 (1H, bs, NH-TZD). ^{13}C NMR (DMSO-d_6, 75 MHz): 115.5, 119.7, 121.7, 123.7, 127.9, 128.0, 128.3, 128.6, 128.7, 130.0, 133.1, 138.9, 147.9, 167.5, 167.9. ESI-*m/z*: 353.94 $[M+H]^+$. Anal. calcd. for $C_{17}H_{11}N_3O_2S_2$: C, 57.77; H, 3.14; N, 11.89. Found: C, 57.82; H, 3.12; N, 11.93%.

5-((3-(2-Bromo-4-methoxyphenyl)-1-phenyl-1*H*-pyrazol-4-yl)-methylene)-thiazolidine-2,4-dione (5c)

Yield = 76%, m.p. 263–265°C, R_f = 0.61. FT-IR (KBr, ν_{max} cm^{-1}): 3365 (NH), 3056, 3041 (C—H, Ar), 1757, 1743 (C═O), 1667 (—CH═C—), 1582 (C═N), 1379 (C—N), 628 (C—Br), 665 (C—S). ^1H NMR (DMSO-d_6, 400 MHz), δ ppm: 3.663 (s, 3H, OCH_3), 7.403–7.425 (t, 1H, Ar—H, *J* = 8.8 Hz), 7.513–7.550 (m, 3H, Ar—H), 7.589–7.611 (d, 2H, Ar—H,

J = 8.8 Hz), 7.626–7.647 (d, 2H, Ar—H, *J* = 8.4 Hz), 7.971 (s, 1H, —CH═C), 8.716 (s, 1H, CH, pyrazole H), 12.553 (bs, 1H, NH-TZD). ^{13}C NMR (DMSO-d_6, 75 MHz): 55.2, 114.9, 115.7, 116.1, 118.3, 119.2, 121.1, 121.9, 128.1, 128.6, 129.2, 131.4, 139.5, 152.7, 159.3, 162.9, 167.4, 167.9. ESI-*m/z*: 457.03 $[M+H]^+$. Anal. calcd. for $C_{20}H_{14}BrN_3O_3S$: C, 52.64; H, 3.09; N, 9.21. Found: C, 52.61; H, 3.07; N, 9.25%.

5-((3-(4-Iodophenyl)-1-phenyl-1*H*-pyrazol-4-yl)methylene)-thiazolidine-2,4-dione (5d)

Yield = 66%, m.p. 247–249°C, R_f = 0.79. FT-IR (KBr, ν_{max} cm^{-1}): 3357 (NH), 3077, 3053 (C—H, Ar), 1759, 1748 (C═O), 1649 (—CH═C—), 1561 (C═N), 1377 (C—N), 653 (C—S), 536 (C—I). ^{1}H NMR (DMSO-d_6, 400 MHz), δ ppm: 7.410–7.428 (t, 1H, Ar—H, *J* = 7.2 Hz), 7.555–7.574 (t, 3H, Ar—H, *J* = 7.6 Hz), 7.619–7.677 (m, 4H, Ar—H), 7.993–8.013 (m, 2H, Ar—H, —CH═C), 8.715 (s, 1H, CH, pyrazole-H), 12.564 (bs, 1H, NH-TZD). ^{13}C NMR (DMSO-d_6, 75 MHz): 96.3, 116.0, 119.8, 121.0, 123.6, 128.0, 128.6, 129.4, 130.0, 130.6, 130.7, 139.1, 152.6, 167.5, 167.9. ESI-*m/z*: 473.86 $[M+H]^+$. Anal. calcd. for $C_{19}H_{12}IN_3O_2S$: C, 48.22; H, 2.56; N, 8.88. Found: C, 48.24; H, 2.61; N, 8.97%.

5-((3-(2,4-Dihydroxyphenyl)-1-phenyl-1*H*-pyrazol-4-yl)-methylene)thiazolidine-2,4-dione (5e)

Yield = 77%, m.p. 221–223°C, R_f = 0.68. FT-IR (KBr, ν_{max} cm^{-1}): 3633 (OH), 3347 (NH), 3069, 3057 (C—H, Ar), 1763, 1739 (C═O), 1662 (—CH═C—), 1548 (C═N), 1371 (C—N), 679 (C—S). ^{1}H NMR (DMSO-d_6, 400 MHz), δ ppm: 6.45 (s, 1H, Ar—H), 6.610–6.812 (d, 1H, Ar—H, *J* = 8 Hz), 7.012–7.563 (m, 6H, Ar—H), 7.861 (s, 1H, —CH═C—), 8.536 (s, 1H, —CH═C—), 9.65 (s, 1H, —OH), 10.96 (s, 1H, —OH), 12.337 (bs, 1H, NH-TZD). ^{13}C NMR (DMSO-d_6, 75 MHz): 106.3, 111.7, 115.4, 115.8, 120.6, 123.7, 127.1, 129.9, 131.0, 135.4, 141.2, 146.6, 150.0, 156.1, 161.7, 167.2, 167.8.ESI-*m/z*: 380.65 $[M+H]^+$. Anal. calcd. for $C_{19}H_{13}N_3O_4S$: C, 60.15; H, 3.45; N, 11.08. Found: C, 60.21; H, 3.41; N, 11.12%.

5-((3-(4-Hydroxy-3-methylphenyl)-1-phenyl-1*H*-pyrazol-4-yl)-methylene)thiazolidine-2,4-dione (5f)

Yield = 59%, m.p. 228–230°C, R_f = 0.79. FT-IR (KBr, ν_{max} cm^{-1}): 3623 (OH), 3349 (NH), 3066, 3051 (C—H, Ar), 1761, 1743 (C═O), 1653 (—CH═C—), 1557 (CN), 1367 (C—N), 673 (C—S). ^{1}H NMR (DMSO-d_6, 400 MHz), δ ppm: 2.35 (s, 3H, CH_3), 6.912–6.933 (d, 2H, Ar—H, *J* = 8.4 Hz), 7.385–7.404 (t, 1H, Ar—H, *J* = 7.6 Hz), 7.422–7.443 (d, 2H, Ar—H, *J* = 8.4 Hz), 7.540–7.552 (m, 3H, Ar—H), 8.038 (s, 1H, —CH═C), 8.636 (s, 1H, CH, pyrazole-H), 9.827 (s, 1H, OH), 12.507 (bs, 1H, NH-TZD). ^{13}C NMR (DMSO-d_6, 75 MHz): 15.7, 115.5, 116.7, 120.1, 122.3, 123.5, 125.1, 127.6, 128.1, 130.2, 130.5, 131.7, 133.0, 139.1, 151.6, 155.3, 167.3, 167.8. ESI-*m/z*: 378.06 $[M+H]^+$. Anal. calcd. for $C_{20}H_{15}N_3O_3S$: C, 63.65; H, 4.01; N, 11.13. Found: C, 63.72; H, 3.98; N, 11.16%.

5-((3-(4-Hydroxy-3-methoxyphenyl)-1-phenyl-1*H*-pyrazol-4-yl)-methylene)thiazolidine-2,4-dione (5g)

Yield = 78%, m.p. 243–245°C, R_f = 0.66. FT-IR (KBr, ν_{max} cm^{-1}): 3644 (OH), 3362 (NH), 3068, 3047 (C—H, Ar), 1761, 1742 (C═O), 1657 (—CH═C—), 1565 (C═N), 1459 (NO_2), 1373 (C—N), 669 (C—S). ^{1}H NMR ($CDCl_3$, 400 MHz), δ ppm: 3.813 (s, 3H, OCH_3), 7.330–7.367 (m, 2H, Ar—H), 7.456 (s, 1H, Ar—H), 7.698–7.718 (d, 2H, Ar—H, *J* = 8 Hz), 7.887–7.919 (m, 2H, Ar—H), 7.967–7.996 (m, 2H, Ar—H, —CH═C), 8.683 (s, 1H, CH, pyrazole-H), 9.535 (s, 1H, OH), 12.534 (bs, 1H, NH-TZD). ^{13}C NMR ($CDCl_3$, 75 MHz): 57.3, 107.5, 115.7, 119.3, 122.0, 125.9, 128.2, 129.4, 129.9, 130.3, 133.0, 139.7, 142.8, 147.8, 148.6, 151.3, 167.4, 167.9. ESI-*m/z*: 394.55 $[M+H]^+$. Anal. calcd. for $C_{20}H_{15}N_3O_4S$: C, 61.06; H, 3.84; N, 10.68. Found: C, 61.10; H, 3.87; N, 10.65%.

5-((3-(2-Chloro-3,4-dihydroxyphenyl)-1-phenyl-1*H*-pyrazol-4-yl)-methylene)-thiazolidine-2,4-dione (5h)

Yield = 68%, m.p. 269–271°C, R_f = 0.67. FT IR (KBr, ν_{max} cm^{-1}): 3656 (OH), 3371 (NH), 3085, 3043 (C—H, Ar), 1765, 1747 (C═O), 1653 (—CHC—), 1577 (C═N), 1361 (C—N), 787 (C—Cl), 644 (C—S). ^{1}H NMR (DMSO-d_6, 400 MHz), δ ppm: 7.421–7.439 (t, 1H, Ar—H, *J* = 7.2 Hz), 7.539–7.612 (m, 2H, Ar—H), 7.757–7.791 (m, 4H, Ar—H), 7.957 (s, 1H, —CH═C), 8.477 (s, 1H, CH, pyrazole-H), 9.231 (s, 1H, OH), 10.219 (s, 1H, OH), 12.520 (bs, 1H, NH-TZD). ^{13}C NMR (DMSO d_6, 75 MHz): 114.6, 116.7, 119.2, 121.3, 123.2, 126.0, 128.3, 129.2, 129.8, 130.4, 131.3, 142.5, 146.2, 148.5, 151.6, 167.1, 167.6. ESI-*m/z*: 414.77 $[M+H]^+$. Anal. calcd. for $C_{19}H_{12}ClN_3O_4S$: C, 55.14; H, 2.92; N, 10.15. Found: C, 55.18; H, 2.90; N, 10.21%.

5-((3-(4-Fluoro-3-methylphenyl)-1-phenyl-1*H*-pyrazol-4-yl)-methylene)thiazolidine-2,4-dione (5i)

Yield = 72%, m.p. 174–176°C, R_f = 0.66. FT-IR (KBr, ν_{max} cm^{-1}): 3348 (NH), 3064, 3057 (C—H, Ar), 1767, 1752 (C═O), 1656 (—CH═C—), 1573 (CN), 1368 (C—N), 1234 (C—F), 654 (C—S). ^{1}H NMR (DMSO-d_6, 400 MHz), δ ppm: 2.61 (s, 3H, CH_3), 7.40–7.422 (t, 3H, Ar—H, *J* = 8.8 Hz), 7.551–7.570 (t, 3H, Ar—H, *J* = 7.6 Hz), 7.663–7.698 (m, 2H, Ar—H), 7.987–8.007 (m, 2H, Ar—H, —CH═C), 8.689 (s, 1H, CH, pyrazole-H), 12.527 (bs, 1H, NH-TZD). ^{13}C NMR (DMSO-d_6, 75 MHz): 17.8, 115.9, 116.5, 119.7, 122.2, 123.2, 124.6, 126.5, 127.9, 128.4, 130.0, 131.1, 131.3, 139.1, 152.9, 164.6, 167.5, 167.9. ESI-*m/z*: 379.93 $[M+H]^+$. Anal. calcd. for $C_{20}H_{14}FN_3O_2S$: C, 63.31; H, 3.72; N, 11.08. Found: C, 63.28; H, 3.77; N, 11.12%.

5-((3-(3,4-Dimethoxyphenyl)-1-phenyl-1*H*-pyrazol-4-yl)-methylene)thiazolidine-2,4-dione (5j)

Yield 59%, m.p. 250–252°C, R_f = 0.71. FT-IR (KBr, ν_{max} cm^{-1}): 3362 (NH), 3077, 3048 (C—H, Ar), 2871 (C—H, OCH_3), 1745, 1723 (C═O), 1675 (—CH═C—), 1566 (C═N), 1361 (C—N), 658 (C—S). ^{1}H NMR (DMSO-d_6, 400 MHz), δ ppm: 3.827 (s, 6H, —OCH_3), 7.098–7.143 (m, 2H, Ar—H), 7.202 (s, 1H, Ar—H), 7.396–7.414 (t, 1H, *J* = 7.2 Hz), 7.548–7.567 (t, 2H, Ar—H, *J* = 7.6 Hz), 7.607 (s, 1H, —CH═C), 7.988–8.008 (d, 2H, Ar—H, *J* = 8 Hz), 8.651 (s, 1H, CH, pyrazole-H), 12.497 (bs, 1H, NH-TZD). ^{13}C NMR (DMSO-d_6, 75 MHz): 56.1, 115.9, 117.6, 119.5, 121.1, 122.8, 126.3, 128.7, 129.0, 129.5, 130.4, 139.1, 146.7, 151.6, 153.8, 159.2, 167.3, 167.8. ESI-*m/z*: 408.27 $[M+H]^+$. Anal. calcd. for $C_{21}H_{17}N_3O_4S$: C, 61.90; H, 4.21; N, 10.31. Found: C, 61.87; H, 4.26; N, 10.33%.

5-((3-(2,4-Dimethoxyphenyl)-1-phenyl-1*H*-pyrazol-4-yl)-methylene)thiazolidine-2,4-dione (5k)

Yield = 55%, m.p. 241–243°C, R_f = 0.57. FT-IR (KBr, ν_{max} cm^{-1}): 3371 (NH), 3079, 3053 (C—H, Ar), 2857 (C—H, OCH_3), 1754, 1736 (C═O), 1673 (—CH═C—), 1577 (C═N), 1365 (C—N), 647 (C—S). ^{1}H NMR (DMSO-d_6, 400 MHz), δ ppm: 3.812 (s, 6H, —OCH_3), 7.116–7.253 (m, 3H, Ar—H), 7.366–7.617 (m, 4H, Ar—H), 7.983–8.005 (m, 2H, Ar—H, —CH═C), 8.636 (s, 1H, CH, pyrazole-H), 12.541 (bs, 1H, NH-TZD). ^{13}C NMR (DMSO-d_6, 75 MHz): 55.3, 56.4, 101.4, 111.7, 119.2, 119.4, 121.3, 126.1, 128.3, 129.1, 129.5, 130.1, 139.2, 146.5, 153.1, 157.6, 159.3, 167.1, 167.5. ESI-*m/z*: 408.11 $[M+H]^+$. Anal. calcd. for $C_{21}H_{17}N_3O_4S$: C, 61.90; H, 4.21; N, 10.31. Found: C, 61.93; H, 4.25; N, 10.36%.

5-((3-(3-Bromo-[1,1′-biphenyl]-4-yl)-1-phenyl-1*H*-pyrazol-4-yl)-methylene)thiazolidine-2,4-dione (5l)

Yield = 62%, m.p. 209–211°C, R_f = 0.76. FT-IR (KBr, ν_{max} cm^{-1}): 3367 (NH), 3077, 3061 (C—H, Ar), 2932 (C—H, CH_3), 1757, 1734 (C═O), 1663 (—CH═C—), 1582 (C═N), 1355 (C—N), 633 (C—Br), 643 (C—S). ^{1}H NMR ($CDCl_3$, 400 MHz), δ ppm: 7.309–7.329 (d, 2H, Ar—H, *J* = 8 Hz), 7.391–7.415 (m, 5H, Ar—H), 7.513–7.532 (t, 2H, Ar—H, *J* = 7.6 Hz), 7.710–7.730 (d, 2H, Ar—H, *J* = 8 Hz), 7.787–7.807 (d, 2H, Ar—H, *J* = 8 Hz), 8.016 (s, 1H, —CH═C), 8.538 (s, 1H, CH, pyrazole-H), 12.508 (bs, 1H, NH-TZD). ^{13}C NMR ($CDCl_3$,75 MHz): 131.4, 119.2, 120.5, 122.3, 126.1, 126.7, 127.2, 127.9, 128.9, 129.4, 129.8, 130.6, 134.5, 138.4, 138.7, 139.3, 141.1, 144.0, 150.6, 167.5, 168.1. ESI-*m/z*: 503.45 $[M+H]^+$. Anal. calcd. for $C_{25}H_{16}BrN_3O_2S$: C, 59.77; H, 3.21; N, 8.36. Found: C, 59.73; H, 3.18; N, 8.41%.

5-((1-Phenyl-3-(pyridin-3-yl)-1*H*-pyrazol-4-yl)-methylene)-thiazolidine-2,4-dione (5m)

Yield = 63%, m.p. 235–237°C, R_f = 0.58. FT-IR (KBr, ν_{max} cm^{-1}): 3379 (NH), 3047, 3031 (C—H, Ar), 1770, 1745 (C═O), 1681 (—CHC—), 1567 (C═N), 1355 (C—N), 667 (C—S). ^{1}H NMR ($CDCl_3$, 400 MHz), δ ppm: 6.679–6.697 (t, 1H, Ar—H, *J* = 7.2 Hz), 6.908–6.944 (d, 2H, Ar—H, *J* = 14.4 Hz), 7.028–7.110 (m, 4H, Ar—H), 7.913–7.933 (d, 2H, Ar—H, *J* = 8 Hz), 8.311 (s, 1H, —CH═C), 8.749 (s, 1H, CH, pyrazole-H), 12.463 (bs, 1H, NH-TZD). ^{13}C NMR ($CDCl_3$, 75 MHz): 115.8, 119.6, 122.6, 123.1, 125.3, 127.1, 130.3, 132.6, 132.9, 133.6, 138.5, 141.7, 147.9, 148.3, 167.1, 167.7. ESI-*m/z*: 349.13 $[M+H]^+$. Anal. calcd. for $C_{18}H_{12}N_4O_2S$: C, 62.06; H, 3.47; N, 16.08. Found: C, 62.02; H, 3.45; N, 16.11%.

5-((3-(4-Isobutylphenyl)-1-phenyl-1*H*-pyrazol-4-yl)methylene)-thiazolidine-2,4-dione (5n)

Yield = 75%, m.p. 221–223°C, R_f = 0.74. FT-IR (KBr, ν_{max} cm^{-1}): 3365 (NH), 3056, 3038 (C—H, Ar), 1773, 1741 (C═O), 1663 (C═C), 1582 (C═N), 1367 (C—N), 642 (C—S). ^{1}H NMR ($CDCl_3$, 400 MHz), δ ppm: 1.238 (s, 6H, CH_3), 1.815 (s, 1H, CH, isobutyl), 2.215 (m, 2H, CH_2, isobutyl), 7.398–7.417 (t, 1H, Ar—H, *J* = 7.6 Hz), 7.460–7.537 (m, 5H, Ar—H), 7.795–7.882 (m, 4H, Ar—H), 8.181 (s, 1H, —CH═C), 8.550 (s, 1H, CH, pyrazole-H), 12.513 (bs, 1H, NH-TZD). ^{13}C NMR ($CDCl_3$, 75 MHz): 23.2, 31.7, 43.3, 115.4, 119.7, 121.8, 126.1, 127.3, 129.0, 129.2, 130.1, 132.8, 139.2, 141.6, 142.9, 149.6, 167.6, 168. ESI-*m/z*: 404.36 $[M+H]^+$. Anal. calcd. for $C_{23}H_{21}N_3O_2S$: C, 68.46; H, 5.25; N, 10.41. Found: C, 68.52; H, 5.21; N, 10.45%.

5-((3-(Naphthalen-2-yl)-1-phenyl-1*H*-pyrazol-4-yl)methylene)-thiazolidine-2,4-dione (5o)

Yield = 69%, m.p. 281–283°C, R_f = 0.81. FT-IR (KBr, ν_{max} cm^{-1}): 3371 (NH), 3058, 3042 (C—H, Ar), 1771, 1747 (C═O), 1672 (—CH═C—), 1579 (C═N), 1375 (C—N), 645 (C—S). ^{1}H NMR ($CDCl_3$, 400 MHz), δ ppm: 7.521–7.956 (m, 12H, Ar—H), 8.256 (s, 1H, —CH═C), 8.656 (s, 1H, CH, pyrazole-H), 12.426 (bs, 1H, NH-TZD). ^{13}C NMR ($CDCl_3$, 100 MHz): 116.2, 120.3, 123.5, 126.1, 126.4, 126.9, 128.8, 129.1, 129.7, 130.2, 130.9, 133.6, 134.4, 141.5, 145.3, 152.8, 167.1, 167.8. ESI-*m/z*: 398.36 $[M+H]^+$. Anal. calcd. for $C_{23}H_{15}N_3O_2S$: C, 69.50; H, 3.80; N, 10.57. Found: C, 69.56; H, 3.83; N, 10.62%.

4.2 | Molecular docking studies

Molecular docking study was carried out to assess their interaction and binding modes with target receptor using Glide 5.5 extra precision (XP) Maestro 10.1 Schrodinger,[38] running on Linux 64 operating system. It comprised of a series of steps which includes selection of protein and its preparation, receptor grid generation, preparation of ligand and its docking to the receptor. Protein with PDB ID-2PRG was downloaded from Protein Data Bank at a resolution of 2.3 Å, which was used in molecular docking studies. Peroxisome proliferator-activated receptor-γ (PPAR-γ) is a nuclear receptor consisting of two monomer chains (A and B). Due to the presence of our TZD moiety in chain A, chain B was deleted along with residual water molecules which were beyond 5 Å, leaving behind water molecules near the ligand to yield energy minimized protein structure. These energy minimized protein structures were then used to generate grid which used reference drug as a ligand to signify the binding sites within the receptor target. The ligand preparation involves 2D or 3D structures and producing their low energy states in Maestro format using OPLS 2005 force field, with the possibilities to extend each input structure by generating variation on ionization states. Finally docking was carried out using Glide software with extra precision and write XP descriptor information. During this procedure, favorable ligand poses were then generated to determine their spatial fit into the active site of receptor and those who fitted best were then evaluated and minimized for generating glide scores. The Glide score, hydrogen bonds, and π–π interaction formed with the surrounding amino acids were used to predict the binding affinities and proper alignment of these compounds at the active site of the receptor or enzyme (Table 1).

4.3 | Biological activity

4.3.1 | *In vitro* PPAR-γ transactivation assay

Human embryonic kidney (HEK) 293 cells were cultured with 10% heat inactivated fetal bovine serum (FBS) in Dulbecco's Modified Eagle's Medium (DMEM) under humid conditions with 5% CO_2 at 37°C. The

TABLE 1 Glide score, Glide energy, and ADME prediction of the synthesized compounds, **5a–o**

Comp.	Glide score	Glide energy	Log Po/w[a]	PSA[b]	Log *S*[c]	Rule of five[d]
5a	−9.363	−73.293	4.712	89.383	−6.755	0
5b	−8.896	−64.599	4.001	88.440	−5.813	1
5c	−5.751	−66.265	4.207	94.932	−5.995	0
5d	−8.153	−69.927	4.688	89.375	−6.784	0
5e	−6.865	−72.633	2.392	130.195	−4.737	0
5f	−8.027	−70.468	3.398	109.976	−5.522	0
5g	−6.407	−73.449	3.142	119.870	−4.980	0
5h	−6.902	−76.981	2.678	130.020	−5.140	0
5i	−8.986	−64.253	4.297	89.377	−6.165	0
5j	−6.962	−69.935	3.889	106.045	−5.350	0
5k	−6.726	−66.977	3.910	102.887	−5.642	0
5l	−8.781	−74.327	5.767	86.452	−7.854	2
5m	−6.496	−58.219	3.059	133.358	−5.600	0
5n	−9.526	−65.668	2.805	102.247	−4.777	0
5o	−9.706	−81.249	4.747	89.372	−6.621	0
Rosiglitazone	−9.165	−87.861	3.594	94.178	−4.988	0

[a]Predicted octanol/water partition coefficient (<5).
[b]Van der Waals surface area of polar nitrogen and oxygen atoms and carbonyl carbon atoms (range 7–200).
[c]Predicted aqueous solubility, log *S*. *S* in mol/dm^3 is the concentration of the solute in a saturated solution that is in equilibrium with the crystalline solid (range −6.5 to 0.5).
[d]Lipinski's violations (≤1).

day before transfection, six-well plates were seeded with cells to give 70–80% confluence at transfection. 96-well plates containing 60000 cells/well were inoculated with cells grown in DMEM and were transfected with 2.5 µL of PPRE-luciferase, 6.67 µL of PPAR-γ, 1.0 µL of Renilla, and 20 µL of lipofectamine. Five hours after transfection, the cells were treated with synthesized analogues (10 µM) for 24 h and then collected with cell culture lysis buffer. Pioglitazone and rosiglitazone were used as reference drug and luciferase activity was monitored using the luciferase assay kit (Promega) on luminometer (Perkin Elmer, USA) according to instructions cited by manufacturer.

4.3.2 | Antidiabetic activity

In vivo antidiabetic study was determined by studying the effects of orally administered different TZD analogues on glucose tolerance in normal and streptozotocin (STZ) induced non-insulin-dependent diabetes mellitus (NIDDM) in rats. Healthy Albino Wistar rats of either sex (180–250 g) were acquired from Central Animal House Facility, Jamia Hamdard, New Delhi, and kept at room temperature with food and water *ad libitum*. STZ was freshly prepared in 0.1 M citrate buffer solution (pH 4.5) for inducing diabetes at a dose of 60 mg/kg body weight intraperitoneally to overnight-fasted rats. To overcome drug-induced hypoglycemia, the animals were permitted to drink only 5% glucose solution whole night. If the blood glucose level of animals was found to be 250 mg/dL or above on third day after STZ injection, they were considered as diabetic. The animals were classified into five groups containing six animals in each group. Group I (control) received 0.1 M citrate buffer, diabetic rats received STZ injection (Group II), diabetic rats orally fed with pioglitazone (as 0.25% CMC suspension) at a dose of 36 mg/kg (Group III), diabetic rats orally fed with rosiglitazone (as 0.25% CMC suspension) at a dose of 36 mg/kg (Group IV), diabetic rats orally fed with synthesized compounds, **5a–o** (as 0.25% CMC suspension) at an equimolar dose of the reference drug pioglitazone (Group V). The blood glucose level of each group was checked at 0, 1, 7, and 15 days through glucose oxidase method. The experiments performed followed the rules of Institutional Animals Ethics Committee (registration number 173-CPCSEA).[39,40]

4.3.3 | Biochemical parameters

Serum aspartate aminotransferase (AST) and alanine aminotransferase (ALT) were performed according to Reitman and Frankel method[41] and alkaline phosphatase (ALP) was assayed according to Walter and Schult method[42] using 4-nitrophenyl phosphate as substrate.

4.3.4 | Hepatotoxicity studies

The hepatotoxicity determination of synthesized analogues was carried out according to the reported method of Lambert et al.[43] The animals were classified into five groups containing six animals in each group. Group I (control) received 0.1 M citrate buffer, diabetic rats received STZ injection at a dose of 60 mg/kg (Group II), diabetic rats orally fed with pioglitazone (as 0.25% CMC suspension) at a dose

of 108 mg/kg (Group III), diabetic rats orally fed with rosiglitazone (as 0.25% CMC suspension) at a dose of 108 mg/kg (Group IV), diabetic rats orally fed with synthesized compounds **5a**, **5b**, **5i**, **5n**, and **5o** (as 0.25% CMC suspension) at an equimolar dose of the reference drug pioglitazone (Group V). After 5 h of the test drug administration in rats at a dose three times higher than the dose for anti-diabetic activity, rats were sacrificed using low level of anesthesia to remove their liver specimens which were then preserved in formalin solution (10%). Morphological examination was conducted to analyze histological changes in liver using hematoxylin and eosin dye staining and then examined under microscope.

4.3.5 | PPAR-γ gene expression study

Cell culture experiments

Twenty-four-well plates were seeded with 3T3-L1 cells (ATCC) 24 h before treatment in DMEM which contains calf serum (10%) (Invitrogen). After 24 h, the cells were then treated with synthesized analogue **5o** (10 μM), pioglitazone and rosiglitazone (reference drug, 10 μM) as positive control and dimethyl sulfoxide (DMSO) as negative control and then incubated in CO_2 incubator for next 24 h with 5% CO_2 at 37°C. The cells were then scraped off and collected in microcentrifuge tubes (1.5 mL) to isolate total RNA using TRI Reagent (Molecular Research Center). Further the quantity and quality of RNA were evaluated on a NanoDrop ND-2000c spectrophotometer and integrity was determined on agarose gel (1.5%). The total RNA (1 μg) so obtained was then used to generate cDNA for reverse transcription-polymerase chain reaction (Biological Industries) using an EZ-first strand synthesis kit for cDNA. Primers for PPAR-γ and β-actin for real-time polymerase chain reaction (PCR) were designed using Pearl Primer software. Real-time PCR was done on ABI Prism 7300 Sequence Detection System (Applied Biosystems) using the SYBR Green PCR Master Mix (Applied Biosystems) and was performed in triplicate and repeated two times for each gene and sample. Reactions were carried out at 95°C for 10 min followed by 40 cycles of 95°C for 15 s and 60°C for 1 min. Relative transcript quantities were calculated using the Ct method with β-actin as endogenous reference gene.[33,34]

ACKNOWLEDGMENTS

The authors are thankful to Jamia Hamdard, New Delhi, India, for providing facilities for research work, spectral and elemental studies. The corresponding author (Dr. Ozair Alam) is also thankful to DST-SERB (SB/FT/LS-203-2012), New Delhi, for providing funds to purchase molecular modeling software (Schrödinger, USA) under Fast track young scientist.

CONFLICT OF INTEREST

The authors declare no conflict of interest.

ORCID

Ozair Alam http://orcid.org/0000-0003-0322-2509
Md. Mumtaz Alam http://orcid.org/0000-0001-6420-8757

REFERENCES

[1] C. Kharbanda, M. S. Alam, H. Hamid, K. Javed, A. Dhulap, S. Bano, Y. Ali, *Bioorg. Med. Chem. Lett*. **2015**, *25*, 4601.
[2] S. Nazreen, M. S. Alam, H. Hamid, M. S. Yar, A. Dhulap, P. Alam, M. A. Pasha, S. Bano, M. M. Alam, S. Haider, C. Kharbanda, *Bioorg. Med. Chem. Lett*. **2014**, *24*, 3034.
[3] D. P. Rotella, *J. Med. Chem*. **2004**, *47*, 4111.
[4] K. Liu, L. Xu, D. Szalkowski, Z. Li, V. Ding, G. Kwei, S. Huskey, D. E. Moller, J. V. Heck, B. B. Zhang, A. B. Jones, *J. Med. Chem*. **2000**, *43*, 3487.
[5] R. Jeon, Y. J. Kim, Y. Cheon, J. H. Ryu, *Arch. Pharm. Res*. **2006**, *29*, 394.
[6] G. M. Reaven, H. Chang, B. B. Hoffman, *Diabetes* **1988**, *37*, 28.
[7] U. Ramachandran, A. Mital, P. V. Bharatam, S. Khanna, P. R. Rao, K. Srinivasan, R. Kumar, H. P. Chawla, C. L. Kaul, S. Raichur, R. Chakrabarti, *Bioorg. Med. Chem*. **2004**, *12*, 655.
[8] R. A. DeFronzo, R. C. Bonadonna, E. Ferrannini, *Diabetes Care* **1992**, *15*, 318.
[9] G. M. Reaven, *Diabetes* **1988**, *37*, 1595.
[10] B. C. Cantello, M. A. Cawthorne, G. P. Cottam, P. T. Duff, D. Haigh, R. M. Hindley, C. A. Lister, S. A. Smith, P. L. Thurlby, *J. Med. Chem*. **1994**, *37*, 3977.
[11] Y. H. Fan, H. Chen, A. Natarajan, Y. Guo, F. Harbinski, J. Iyasere, W. Christ, H. Aktas, J. A. Halperin, *Bioorg. Med. Chem. Lett*. **2004**, *14*, 2547.
[12] H. N. Hafez, A. R. El-Gazzar, *Bioorg. Med. Chem. Lett*. **2009**, *19*, 4143.
[13] K. A. Reddy, B. B. Lohray, V. Bhushan, A. S. Reddy, P. H. Kishore, V. V. Rao, V. Saibaba, A. C. Bajji, B. M. Rajesh, K. V. Reddy, R. Chakrabarti, *Bioorg. Med. Chem. Letts*. **1998**, *8*, 999.
[14] C. G. Bonde, N. J. Gaikwad, *Bioorg. Med. Chem*. **2004**, *12*, 2151.
[15] C. Prabhakar, G. Madhusudhan, K. Sahadev, C. M. Reddy, M. R. Sarma, G. O. Reddy, R. Chakrabarti, C. S. Rao, T. D. Kumar, R. Rajagopalan, *Bioorg. Med. Chem. Lett*. **1998**, *8*, 2725.
[16] N. Sunduru, K. Srivastava, S. Rajakumar, S. K. Puri, J. K. Saxena, P. M. Chauhan, *Bioorg. Med. Chem. Lett*. **2009**, *19*, 2570.
[17] V. Patil, K. Tilekar, S. Mehendale-Munj, R. Mohan, C. S. Ramaa, *Eur. J. Med. Chem*. **2010**, *45*, 4539.
[18] Y. Wu, H. H. Tai, H. Cho, *Bioorg. Med. Chem*. **2010**, *18*, 1428.
[19] O. Bozdağ-Dündar, B. Evranos, N. Daş-Evcimen, M. Sarıkaya, R. Ertan, *Eur. J. Med. Chem*. **2008**, *43*, 2412.
[20] B. R. Bhattarai, B. Kafle, J. S. Hwang, S. W. Ham, K. H. Lee, H. Park, I. O. Han, H. Cho, *Bioorg. Med. Chem. Lett*. **2010**, *20*, 6758.
[21] R. Mohan, A. K. Sharma, S. Gupta, C. S. Ramaa, *Med. Chem. Res*. **2012**, *21*, 1156.
[22] Y. M. Ha, Y. J. Park, J. A. Kim, D. Park, J. Y. Park, H. J. Lee, J. Y. Lee, H. R. Moon, H. Y. Chung, *Eur. J. Med. Chem*. **2012**, *49*, 245.
[23] C. Zhou, C. Tang, E. Chang, M. Ge, S. Lin, E. Cline, C. P. Tan, Y. Feng, Y. P. Zhou, G. J. Eiermann, A. Petrov, *Bioorg. Med. Chem. Lett*. **2010**, *20*, 1298.
[24] J. Feng, Y. Lu, Z. F. Cai, S. P. Zhang, Z. R. Guo, *Chinese Chem. Lett*. **2007**, *18*, 45.
[25] T. M. Willson, P. J. Brown, D. D. Sternbach, B. R. Henke, *J. Med. Chem*. **2000**, *43*, 527.
[26] S. Kersten, B. Desvergne, W. Wahli, *Nature* **2000**, *405*, 421.
[27] G. Lee, F. Elwood, J. McNally, J. Weiszmann, M. Lindstrom, K. Amaral, M. Nakamura, S. Miao, P. Cao, R. M. Learned, J. L. Chen, *J. Biol. Chem*. **2002**, *277*, 19649.
[28] C. Pirat, A. Farce, N. Lebègue, N. Renault, C. Furman, R. Millet, S. Yous, S. Speca, P. Berthelot, P. Desreumaux, P. Chavatte, *J. Med. Chem*. **2012**, *55*, 4027.

[29] A. S. Wagman, J. M. Nuss, *Curr. Pharm. Des*. **2001**, *7*, 417.
[30] H. K. Rami, S. A. Smith, *Expert Opin. Ther. Pat*. **2000**, *10*, 623.
[31] S. P. Gupta, *Springer Berlin Heidelberg* **2006**, *3*, 153.
[32] V. A. Dixit, P. C. Rathi, S. Bhagat, H. Gohlke, R. K. Petersen, K. Kristiansen, A. K. Chakraborti, P. V. Bharatam, *Eur. J. Med. Chem*. **2016**, *108*, 423.
[33] N. K. LeBrasseur, M. Kelly, T. S. Tsao, S. R. Farmer, A. K. Saha, N. B. Ruderman, E. Tomas, *Am. J. Physiol. Endocrinol. Metab*. **2006**, *29*, E175.
[34] Z. Wu, E. D. Rosen, R. Brun, S. Hauser, G. Adelmant, A. E. Troy, C. McKeon, G. J. Darlington, B. M. Spiegelman, *Mol. Cell*. **1999**, *3*, 151.
[35] J. J. Vora, S. B. Vasava, K. C. Parmar, S. K. Chauhan, S. S. Sharma, *J. Chem*. **2009**, *6*, 1205.
[36] O. Prakash, D. K. Aneja, S. Arora, C. Sharma, K. R. Aneja, *Med. Chem. Res*. **2012**, *21*, 10.
[37] a) N. C. Desai, H. M. Satodiya, K. M. Rajpara, V. V. Joshi, K. Bhatt, H. V. Vaghani, Anti-Infect. Agents 2014, 12, 85; b) N. C. Desai, H. M. Satodiya, G. M. Kotadiya, H. V. Vaghani, Arch. Pharm. Chem. Life Sci. 2014, 347, 523.
[38] Schrödinger. Maestro version 10.1 [software] New York: Schrödinger; **2016**.
[39] A. Dahlqvist, *Biochem. J*. **1961**, *80*, 547.
[40] S. Nazreen, M. S. Alam, H. Hamid, M. Shahar Yar, S. Shafi, A. Dhulap, P. Alam, M. A. Q. Pasha, S. Bano, M. M. Alam, S. Haider, C. Kharbanda, Y. Ali, K. K. Pillai, *Eur. J. Med. Chem*. **2014**, *87*, 175.
[41] S. Reitman, S. Frankel, *Am. J. Clin. Pathol*. **1957**, *28*, 56.
[42] K. Walter, C. Schult Bergmeyer (Eds.), *Methods of Enzymatic Analysis*, Academic Press, New York **1974**, pp. 356–360.
[43] J. D. Lambert, M. J. Kennett, S. Sang, K. R. Reuhl, J. Ju, C. S. Yang, *Food Chem. Toxicol*. **2010**, *48*, 409.

SUPPORTING INFORMATION

Additional Supporting Information may be found online in the supporting information tab for this article.

How to cite this article: Naim MJ, Alam O, Alam MJ, Shaquiquzzaman M, Alam MM, Naidu VGM. Synthesis, docking, *in vitro* and *in vivo* antidiabetic activity of pyrazole-based 2,4-thiazolidinedione derivatives as PPAR-γ modulators. *Arch Pharm Chem Life Sci*. 2018;1–15. https://doi.org/10.1002/ardp.201700223